

## Charge/discharge Profiling of Organic Latent Heat Material Embedded in Polymer Matrix for Heat Energy System

Reza Abdu RAHMAN<sup>1,2</sup>, Sulistyو SULISTYO<sup>1\*</sup>, M. S. K. Tony Suryo UTOMO<sup>1</sup>,  
Ilham FEBRIANSYAH<sup>2</sup>, Ismail ISMAIL<sup>2</sup>

<sup>1</sup> Department of Mechanical Engineering, Universitas Diponegoro, Semarang 50275, Indonesia

<sup>2</sup> Department of Mechanical Engineering, Faculty of Engineering, Universitas Pancasila, DKI Jakarta 12640, Indonesia

<http://doi.org/10.5755/j02.ms.36328>

Received 13 February 2024; accepted 16 May 2024

The operational aspect of a latent thermal energy storage (LTES) system is highly dependent on the performance of its latent heat storage material (LHSM). In this work, performance evaluation of the LHSM is conducted using low-density polyethylene (LDPE) and linear LDPE. As an initial assessment, three different organic LHSMs are used for the evaluation. The thermal assessment indicates that the heat of fusion for the LHSM varies between 142.45 J/g and 198.8 J/g. Thermal decomposition demonstrates that the LHSM is suitable for operating a thermal power system under 100 °C. The addition of polymer clearly influences the charge/discharge rate for each LHSM. For example, it has a positive influence on paraffin wax, which increases the charge rate up to 54.4 %. A positive outcome is also observed for palmitic acid, which has the highest charge rate at around 4.4 °C/min. Interestingly, the charge/discharge rate for stearic acid is decreased by the presence of a polymer. It implies that the melting/solidification rate can be decreased, which may be advantageous for passive thermal systems. In general, the addition of LDPE/LLDPE alters the performance of LHSM. It makes the polymer suitable to be taken as a stabilizer for the LHSM.

*Keywords:* polymer, latent heat, energy, power, heat.

### 1. INTRODUCTION

The requirement for a reliable energy system, primarily one that operates in a renewable system, should be accompanied by a suitable energy storage system (ESS). The high development of the ESS can be recognized in the achievement of the battery for electrical storage [1]. Current development is also focused on different models of ESS, such as thermal energy storage (TES), to accommodate the variation in the energy system which generally operates using a solar thermal system [2]. Besides the energy sector, the recent global issue comes from waste, which is a direct result of rapid population growth [3]. The major contribution of the waste is obtained as plastic (LDPE & LLDPE), a polymer substance that has an important role in modern society [4]. It makes the recycling and reutilization of polymer waste attract researchers' attention, especially to the application of energy storage technology that is expected to improve its performance [5].

The role of the TES system in the current energy model is exceptionally critical [6]. It makes improving the material for TES mandatory to achieve a better operational consideration for its application. The most advanced material is sensible TES (STES), already reaching the final commercialization stage and is widely applied in various energy sectors [7]. Unfortunately, the low energy density limits its application, especially for mobile and compacted energy systems. As an alternative, the latent TES (LTES) is chosen. It operates by harvesting the heat energy from latent heat storage material (LHSM) during phase change [8]. The proposed concept increases the energy density of TES,

which makes current development focused on improving the power and performance of the LTES system [9].

The LHSM has several categories, such as inorganic salt, which is generally suitable for operating a medium-temperature LTES system above 100 °C [10]. For low-heat temperatures, which operate between 50–100 °C, the utilization of organic LHSM is highly recommended [11–13]. It is suitable for many heat energy systems, including renewable dryer systems [14], room [15], and water heaters [16]. The organic LHSM has many critical benefits: high enthalpy and considerably low cost. It motivates the utilization of LHSM as a reliable LTES material [17]. However, some technical problems are found in the utilization of LHSM in the LTES system.

The solution to resolve the technical issues is addressed specifically for the operational aspect of the storage tank for an LTES system. The system operates as a heat exchanger [18]. Several studies have reported some development in the storage unit. For example, modification by utilizing the coil arrangement has been proven to improve the power performance of the LTES system [19]. For the air heater system, advancement is taken through optimization in a double-pass system model [20]. Applying nanoparticles in the working fluid brings positive outcomes regarding the power rate, which significantly improved up to 30 % [21]. The innovation is also introduced for the LTES system through the designation of a cascaded tank [22], adjustment on the effective fin configuration [23], and microchannel [24]. Therefore, the technical issues for the storage tank are

\* Corresponding author. Tel.: +62-24-7460059.

E-mail: [sulistyو@lecturer.undip.ac.id](mailto:sulistyو@lecturer.undip.ac.id) (S. Sulistyو)

generally taken and current development can be focused on the material aspect of the LTES system.

Enhancement of the material of the LTES system can be focused on improving conductivity and phase change behavior. Increasing the conductivity allows the LHSM to achieve a higher power rate. It is done by embedding the solid additives and metal foam on the LHSM [25]. Providing a stable phase change behavior for organic LHSM is conducted by utilizing an additional matrix as a stabilizer. M. He et al. utilized aerogel for organic LHSM (paraffin wax), which showed a notable outcome in accelerating the photothermal conversion [26]. M. Sawadogo et al. synthesized a stable matrix from eco-friendly material and demonstrated compatibility with a higher latent heat of more than 50 J/g [27]. Alternative materials such as polymers are considerably effective as stabilizers, which increase the power performance of the organic LHSM [28].

The phase stabilizer, which comes from a polymer, generally uses high-density polyethylene (HDPE) [29]. Different polymers, such as low-density polyethylene (LDPE) and linear-LDPE (LLDPE), can be considered alternative binders. For example, Y. Lv et al. studied the proposed model for operating LHSM in a thermal management system [30]. The same approach was also studied for conductivity enrichment [31]. It indicates the possibility for further evaluation of the polymer for different organic LHSMs. Moreover, the utilization of the polymer will bring positive influence to overcome the waste problem while at the same time improving the effective power performance of the LTES system.

The present work performs an initial assessment of the charge/discharge behavior of the organic LHSM with the addition of polymer. The charge/discharge behavior is an essential parameter to determine the power performance of the LTES system. The assessment aims to provide a fundamental basis for improving the operational aspect of organic LHSM for the LTES system. The assessment is performed using three different organic LHSMs commonly used in the low-temperature LTES system to provide a comprehensive evaluation. Moreover, the ratio of each polymer type is varied to understand its role in the charge/discharge behavior of the LHSM.

## 2. MATERIALS AND METHOD

Table 1 displays the prepared samples for performance comparison. Each material was purchased from a local supplier as market grade. For the base material, several characterizations were taken to evaluate its properties. Each property can be used to determine the basic properties of each LHSM to support the analysis from performance characterization [32]. The mixture of LHSM and polymer was prepared through the hot blending method [33]. In this process, the polymer was gradually added to the liquid LHSM. It allows for the direct impregnation between the polymer and LHSM, which was helped by mechanical stirring. When the mixture was correctly blended, it was stored at room temperature for solidification. The method is relatively simple, attracting possible large-scale manufacturing methods [34].

Performance characterization was taken by evaluating the charge/discharge behavior of the prepared sample. The

process was done by recording the temperature of the sample during the heating stage (Fig. 1).

**Table 1.** Prepared samples for performance comparison (wt.%)

| Base material | LHSM (pure)       | Polymer 1 (LDPE) |      |      | Polymer 2 (LLDPE) |      |      |
|---------------|-------------------|------------------|------|------|-------------------|------|------|
|               |                   | 5 %              | 10 % | 15 % | 5 %               | 10 % | 15 % |
| Paraffin      | LHSM <sub>1</sub> | ✓                | ✓    | ✓    | ✓                 | ✓    | ✓    |
| Stearic       | LHSM <sub>2</sub> | ✓                | ✓    | ✓    | ✓                 | ✓    | ✓    |
| Palmitic      | LHSM <sub>3</sub> | ✓                | ✓    | ✓    | ✓                 | ✓    | ✓    |

The heating stage was done by heating the sample within the container at 30 watts. The temperature of the sample was recorded. It allows to estimate the charge rate of the sample [35]. The non-load test was chosen for the discharge process. It was aimed to observe the nature of behavior of the prepared sample. The released energy can be further evaluated to determine the suitable tank arrangement and solid enrichment. The charge and discharge behavior can be determined from the measurement, which is essential to consider the power effects of the LHSM in the LTES system.

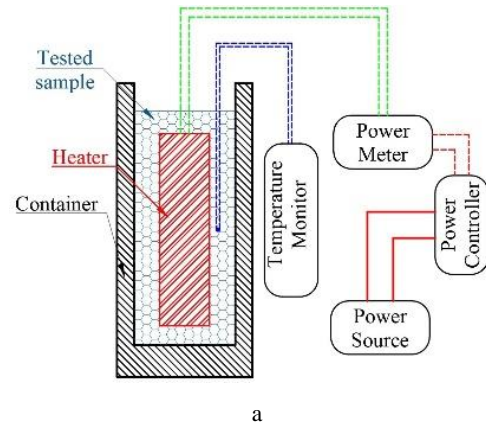


**Fig. 1.** The apparatus for operation evaluation of LHSM as LTES: a – schematic; b – photograph

## 3. RESULTS AND DISCUSSION

Fig. 2 a shows the phase characteristics and melting temperature during the solid-liquid transition of the LHSM, which is used as the base material in this work. The melting behavior of LHSM<sub>1</sub> indicates the two consecutive peaks. It

implies that the phase transition of the LHSM<sub>1</sub> occurs gradually before fully melting. The highest peak of LHSM<sub>1</sub> arises at a temperature 59.16 °C with a total enthalpy of 142.45 J/g. The phase transition behavior of LHSM<sub>2</sub> and LHSM<sub>3</sub> have an identical pattern. It demonstrates a direct melting behavior that appears as a single peak. However, the melting peak for both LHSMs is different. The melting peak for LHSM<sub>2</sub> is observed at 56.01 °C while the LHSM<sub>3</sub> is at 61.62 °C. The differences follow the change in melting peak in enthalpy, where LHSM<sub>2</sub> has a lower enthalpy (148.67 J/g) compared to LHSM<sub>3</sub> (198.8 J/g).

The solidification behavior occurs oppositely and is plotted in Fig. 2 b. All LHSM in this work demonstrate a lower freezing point compared to its melting peak. The supercooling characteristic of the evaluated LHSM is clearly demonstrated due to significant deviation between the phase transition temperature [36]. The freezing peak for LHSM<sub>1</sub> is obtained at 54.1 °C, while LHSM<sub>2</sub> and LHSM<sub>3</sub> occurred at 47.3 °C and 53.3 °C, respectively. According to the result, LHSM<sub>2</sub> and LHSM<sub>3</sub> tend to have a higher supercooling degree. It is affected by the chemical composition of LHSM<sub>2</sub> and LHSM<sub>3</sub>, which is defined as fatty acids.

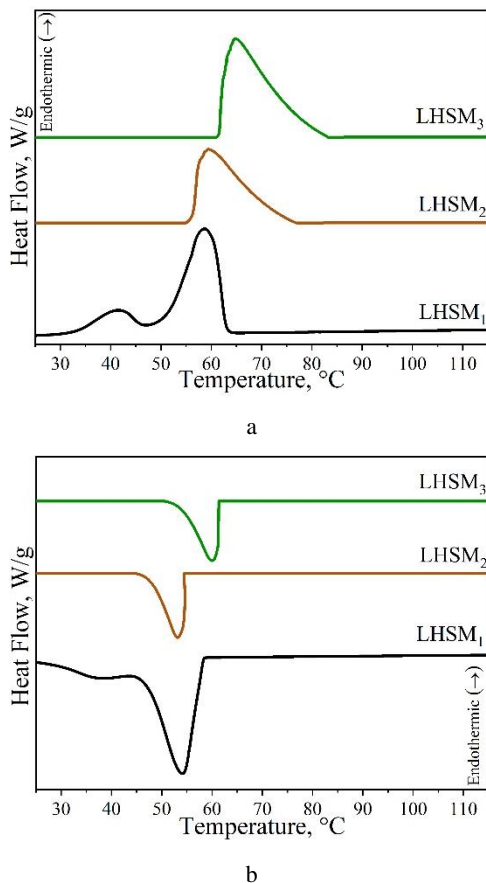


**Fig. 2.** Characteristics from DSC measurement: a –melting; b –freezing

The operational aspect of LTES is defined according to its charge and discharge performance. Thus, the characteristics of the operation of the evaluated LHSM are plotted according to the temperature changes and duration of the charge/discharge process. As plotted in Fig. 3, all LHSMs have a distinctive profile. It implies that each category of LHSM has its characteristics for absorbing and

releasing heat energy. Moreover, the profile confirms the actual performance of the LHSM, which is highly related to the heat exchange process during the operation. Therefore, the profile is addressed as an essential parameter for observing the critical performance of the LHSM in the LTES system.

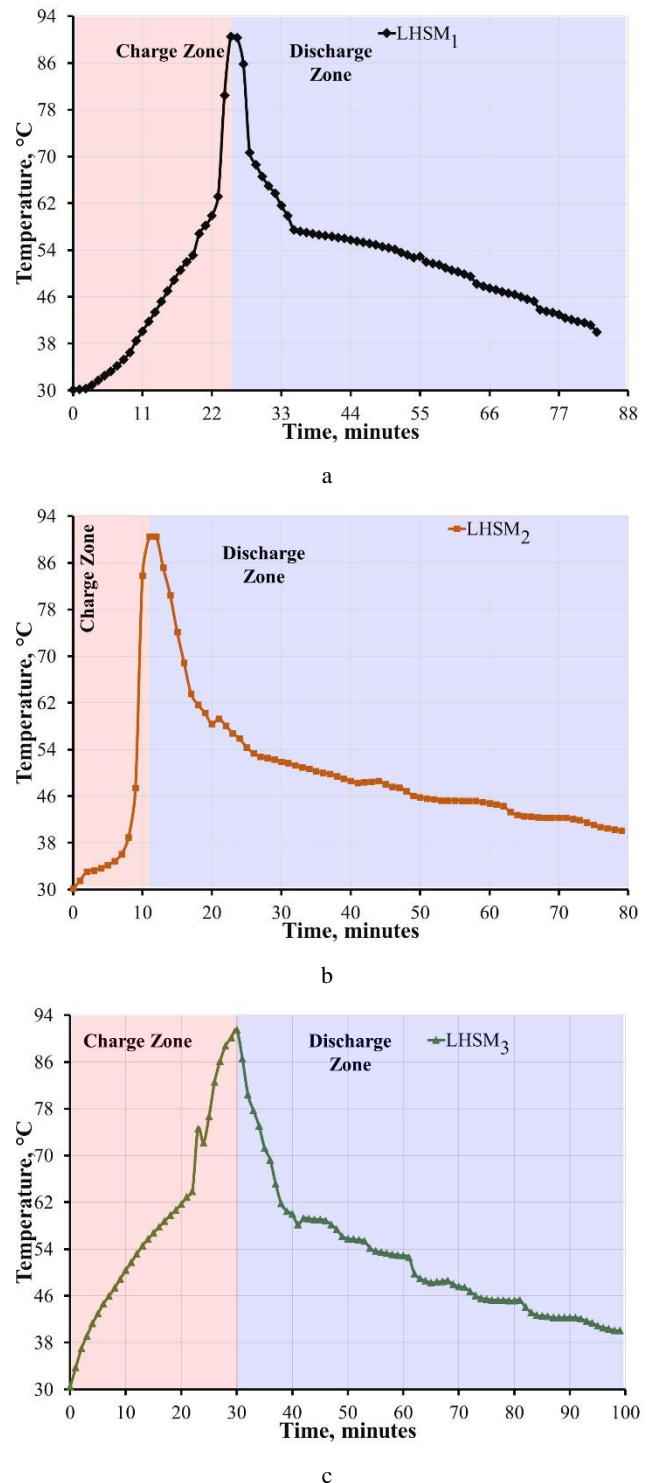


**Fig. 3.** Charge and discharge behavior for the evaluated samples: a –LHSM<sub>1</sub>; b –LHSM<sub>2</sub>; c –LHSM<sub>3</sub>

The heat absorbed for the LHSM<sub>1</sub> demonstrated a short-range phase transition profile that takes place between 53.1 °C and 60.7 °C (Fig. 3 a). The process is done within 3 minutes. According to the DSC profile (Fig. 2 a), the

deceleration in the phase transition region is highly related to the heat absorption for phase change of the LHSM<sub>1</sub>. After passing this stage, the temperature increases notably. The average temperature rate for this stage is obtained at 14.15 °C/min. The phase of the LHSM<sub>1</sub>, which is already in the liquid state, affects the high charge rate. In contrast, the heat is discharged slowly for LHSM<sub>1</sub> due to a low solidification rate. It is the major drawback of the LHSM<sub>1</sub> as in the LTES system since the discharged heat is considered an important parameter of the operational aspect of TES.

The effect of liquid state is also observed for the LHSM<sub>2</sub>. It shows the high-temperature increment for the LHSM<sub>2</sub> once it enters the liquid state (Fig. 3 b). The average rate for LHSM<sub>2</sub> is considerably high, reaching a charge rate of 5.26 °C/min. A lower melting temperature for LHSM<sub>2</sub> influences the high charge rate. Also, the low melting enthalpy affects the amount of heat to change its phase, resulting in a substantial temperature rate during solid-liquid transformation. Despite that, the same behavior is observed according to the discharge profile. It has a rapid freezing stage in the liquid state and liquid-solid region. The heat exchange process is heavily disturbed, especially for the region after solidification. It has a low cumulative discharge rate of less than 0.5 °C/min.

The charge pattern for LHSM<sub>3</sub> is observed at an extended duration, making it the longest charge duration compared to the other LHSM. The total duration to reach the targeted temperature is 29 minutes (Fig. 3 c). The main factor affecting this phenomenon is the high melting temperature of LHSM<sub>3</sub>, followed by the highest melting enthalpy. As a result, it requires a substantial amount of heat energy during solid-liquid transition. The high heat energy content also influenced the heat release behavior. It has the longest discharge behavior, followed by a rapid freezing stage in the early discharge process. One significant performance is observed for LHSM<sub>3</sub>, which is only slightly longer than LHSM<sub>2</sub>. It confirms a better thermal behavior for LHSM<sub>3</sub> than LHSM<sub>2</sub> even though both LHSMs are taken as the same category.

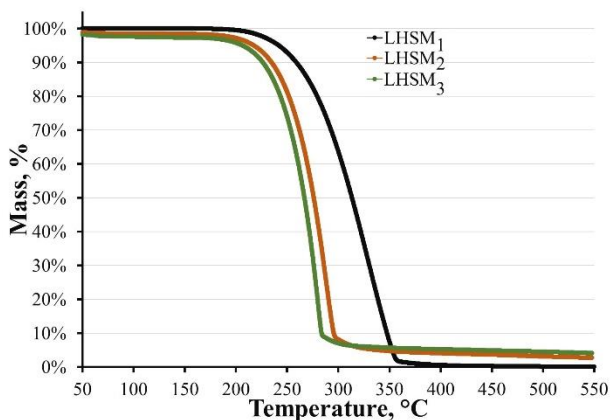


**Fig. 4.** Mass loss profile for the LHSM from thermogravimetric analysis

The thermal decomposition pattern for the LHSM is presented in Fig. 4. The profile reveals crucial information regarding the material's reliability in the LTES system application. All LHSM indicate a direct mass loss profile at

different temperature spans. The decomposition stage for LHSM<sub>1</sub> occurs between 198 °C and 356 °C. Interestingly, the LHSM<sub>2</sub> and LHSM<sub>3</sub> show a similar starting point for the decomposition process. Both LHSMs start to decompose at temperatures of 188 °C to 192 °C. However, the final temperature for LHSM<sub>2</sub> is slightly higher than LHSM<sub>3</sub>. The final temperature for LHSM<sub>2</sub> is observed at 294 °C while LHSM<sub>3</sub> is only 281 °C. Despite the variation in the decomposition range, all LHSMs confirm suitability for operating low-temperature LTES systems. The decomposition is less than 5 % up to a temperature of 150 °C.

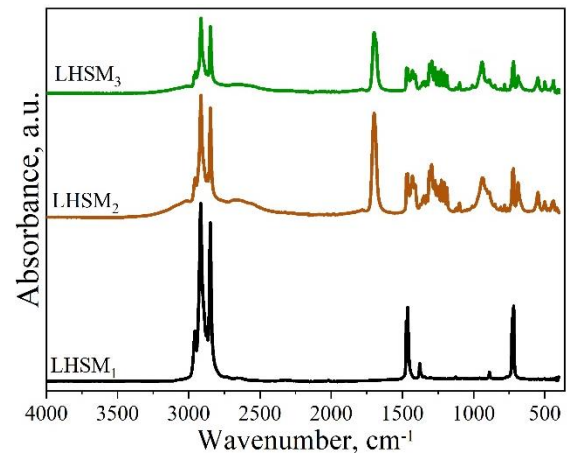


**Fig. 5.** Spectrum FTIR profile for the evaluated LHSM

The chemical composition of the LHSM is evaluated according to the FTIR spectrum. As shown in Fig. 5, each LHSM has a significant pattern that implies its chemical characteristic. First, there is a similar pattern for the first peak, which appears for all LSHM. It is described as a stretching vibration of -CH<sub>2</sub> observed at a wavelength between  $2.9-2.8 \times 10^3 \text{ cm}^{-1}$ . The deformation of the functional group (-CH<sub>2</sub> and -CH<sub>3</sub>) occurs for the LHSM<sub>1</sub> at a specific wavelength range ( $1.48-1.44 \times 10^3 \text{ cm}^{-1}$ ), while the rocking vibration of -CH<sub>2</sub> is observed at  $7.4-7.1 \times 10^3 \text{ cm}^{-1}$ . Specifically, the appearance of stretching C=O at wavelength  $1.7 \times 10^3 \text{ cm}^{-1}$  is taken as the main difference between the category of LHSM<sub>2</sub> and LHSM<sub>3</sub> with LHSM<sub>1</sub>. It confirms the uniqueness of chemical characteristics for each LHSM.

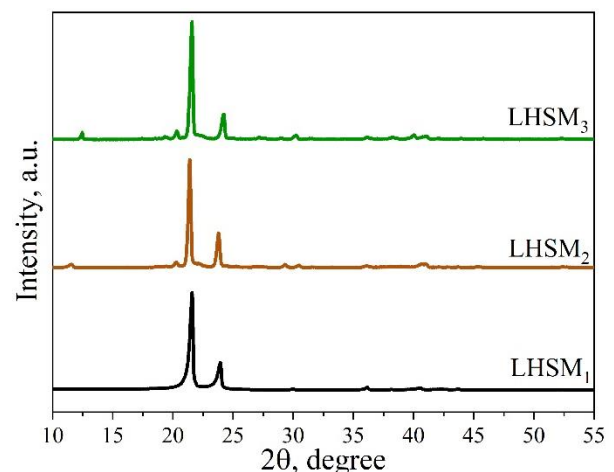


**Fig. 6.** XRD patterns for the evaluated LHSM

Structural analysis is determined according to the XRD pattern. As presented in Fig. 6, all LHSMs have two sharp principal peaks. The principal peak for LHSM<sub>1</sub> is observed at 21.6° and 23.94°. Compared to the FTIR spectra, the LHSM<sub>2</sub> and LHSM<sub>3</sub> have an identical peak with LHSM<sub>1</sub>. The first principal peak for LHSM<sub>2</sub> and LHSM<sub>3</sub> is the same observed at 21.6°. The second peak for LHSM<sub>2</sub> is found at 23.78° while LHSM<sub>3</sub> at 24.2°. Furthermore, a sharp peak indicates the crystalline structure of the LHSM.

The change in the operation characteristic is observed to be notable for all LHSM after the addition of a polymer. As plotted in Fig. 7 a, LHSM<sub>1</sub> has a relatively lower charge rate before the addition of a stabilizer.

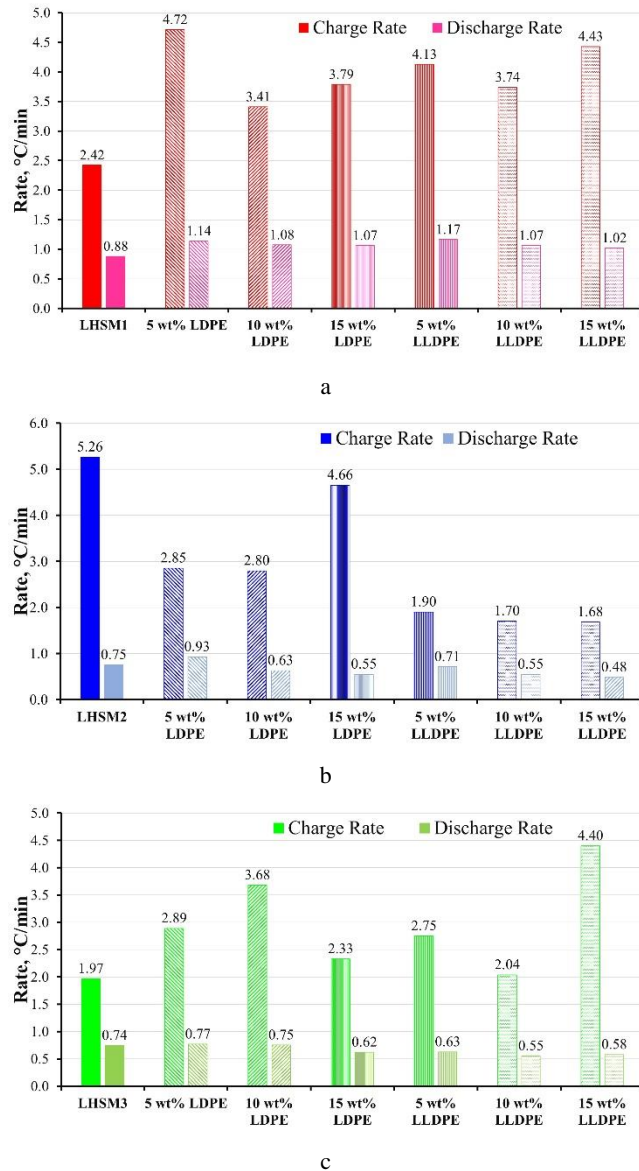


**Fig. 7.** The comparison of charge/discharge behavior for the evaluated samples: a – LHSM<sub>1</sub>; b – LHSM<sub>2</sub>; c – LHSM<sub>3</sub>

It confirms the positive influence of the addition stabilizer for the LHSM<sub>1</sub>. One typical result is obtained for the ratio of 10 wt.% polymer, which has the lowest charge rate compared to the other ratio. For example, 10 wt.% LDPE and LLDPE for LHSM<sub>1</sub> increase the charge rate at ratios around 40.7 % and 54.4 %. The positive influence is also observed notable for the discharge characteristic. The

LHSM<sub>1</sub> with polymer has a better discharge rate, which improved around 29.3 % – 20.8 % (with LDPE) and 32.3 % – 16.1 % (with LLDPE).

The effect of polymer for LHSM<sub>2</sub> is relatively complex compared to LHSM<sub>1</sub> (Fig. 7 b). It is taken as a significant drawback where the presence of both polymers reduces the charge rate. The lowest decrement is obtained for the ratio of 15 wt.% LDPE, where the charge rate decreased by 0.6 °C/min. The decrement is highly associated with the low melting temperature and enthalpy of LHSM<sub>2</sub> according to DSC results (Fig. 2 a). It affects the heat transfer process within the mixture after the addition of the polymer. Moreover, the same condition is also observed for the discharge rate of LHSM<sub>2</sub> with polymer. It can be said that the presence of polymer for LHSM<sub>2</sub> changes the heat exchange process. It reduces the melting and solidification rate of LHSM<sub>2</sub>.

The positive outcome for adding LDPE/LLDPE to fatty acid is observed notable for the LHSM<sub>3</sub> (Fig. 7 c). It significantly improves the average charge rate for the LHSM<sub>3</sub> with polymer, specifically with 10 wt.% LDPE and 15 wt.% LLDPE. The high melting enthalpy followed by a high melting temperature can be taken as a factor that contributes beneficially to the addition of the polymer. It confirms the opposite result for LHSM<sub>2</sub>, which shows a significant change in the charge/discharge rate after adding the polymer. Contrary to the charge rate, the discharge rate generally decreases with the lowest point obtained after adding 10 wt% LLDPE. In this case, the slow solidification rate for LHSM<sub>3</sub> may be taken as a positive impact due to the high melting temperature and enthalpy for LHSM<sub>3</sub>.

#### 4. CONCLUSIONS

The utilization of LDPE and LLDPE for LHSM shows significant changes in its performance. The charge/discharge rate alters notably for the LHSM with LDPE/LLDPE. It improves the operational aspect of LHSM, which comes from paraffin wax and palmitic acid. Despite the considerable decrease in stearic acid, the changes in charge/discharge rate can be adjusted for specific applications that require slow melting and solidification rates. The key result from this work is the potential utilization of LDPE/LLDPE to improve the power performance of LHSM in the LTES system. The polymer itself can be derived from waste. As a result, power performance for LHSM can be adjusted precisely. Further work is still required to apply the detailed evaluation and the application of LHSM/polymer for the TES system.

#### REFERENCES

1. Anseán, D., González, M., Viera, J.C., García, V.M., Blanco, C., Valledor, M. Fast Charging Technique for High Power Lithium Iron Phosphate Batteries: A Cycle Life Analysis *Journal of Power Sources* 239 2013: pp. 9–15. <https://doi.org/10.1016/j.jpowsour.2013.03.044>
2. Suyitno, B.M., Rahman, R.A., Sukma, H., Rahmalina, D. The Assessment of Reflector Material Durability for Concentrated Solar Power Based on Environment Exposure and Accelerated Aging Test *Eastern-European Journal of Enterprise Technologies* 6 2022: pp. 22–29. <https://doi.org/10.15587/1729-4061.2022.265678>

3. **Firman, L.O.M., Adji, R.B., Ismail, I., Rahman, R.A.** Increasing the Feasibility and Storage Property of Cellulose-Based Biomass by Forming Shape-Stabilized Briquette with Hydrophobic Compound *Case Studies in Chemical and Environmental Engineering* 8 2023: pp. 100443. <https://doi.org/10.1016/j.cscee.2023.100443>
4. **Jaiswal, P.B., Pushkar, B.K., Maikap, K., Mahanwar, P.A.** Abiotic Aging Assisted Bio-Oxidation and Degradation of LLDPE/LDPE Packaging Polyethylene Film by Stimulated Enrichment Culture *Polymer Degradation and Stability* 206 2022: pp. 110156. <https://doi.org/10.1016/j.polymdegradstab.2022.110156>
5. **Song, B., Cooke-Willis, M., Theobald, B., Hall, P.** Producing a High Heating Value and Weather Resistant Solid Fuel Via Briquetting of Blended Wood Residues and Thermoplastics *Fuel* 283 2021: pp. 119263. <https://doi.org/10.1016/j.fuel.2020.119263>
6. **Khademi, A., Mehrjardi, S.A.A., Tiari, S., Mazaheri, K., Shafii, M.B.** Thermal Efficiency Improvement of Brayton Cycle in the Presence of Phase Change Material *International Conference on Fluid Flow, Heat and Mass Transfer* 2022: pp. 1–9. <https://doi.org/10.11159/ffhmt22.135>
7. **D'Aguanno, B., Karthik, M., Grace, A.N., Floris, A.** Thermodynamic Properties of Nitrate Molten Salts and Their Solar and Eutectic Mixtures *Scientific Reports* 8 2018: pp. 1–15. <https://doi.org/10.1038/s41598-018-28641-1>
8. **Khademi, A., Darbandi, M., Shafii, M.B., Schneider, G.E.** Numerical Simulation of Thermal Energy Storage Process Benefiting from the Phase Change Materials Concept *AIAA Propulsion and Energy Forum and Exposition* 2019: pp. 1–9. <https://doi.org/10.2514/6.2019-4225>
9. **Khademi, A., Darbandi, M., Schneider, G.E.** Numerical Study to Optimize the Melting Process of Phase Change Material Coupled with Extra Fluid *AIAA Scitech Forum* 1 PartF 2020: pp. 1–6. <https://doi.org/10.2514/6.2020-1932>
10. **Muliawan, B.M., Anggrainy, R., Plamonia, N., Rahman, R.A.** Preliminary Characterization and Thermal Evaluation of a Direct Contact Cascaded Immiscible Inorganic Salt/High-Density Polyethylene as Moderate Temperature Heat Storage Material *Results in Materials* 19 2023: pp. 100443. <https://doi.org/10.1016/j.rinma.2023.100443>
11. **He, Q., Fei, H., Zhou, J., Du, W., Pan, Y., Liang, X.** Preparation and Characteristics of Lauric Acid-Myristic Acid-Based Ternary Phase Change Materials for Thermal Storage *Materials Today Communications* 32 2022: pp. 104058. <https://doi.org/10.1016/j.mtcomm.2022.104058>
12. **Khademi, A., Favakeh, A., Darbandi, M., Shafii, M.B.** Numerical and Experimental Study of Phase Change Material Melting Process in an Intermediate Fluid *7th International Conference on Energy Research and Development (ICERD)* 2019: pp. 16–23.
13. **Favakeh, A., Khademi, A., Shafii, M.B.** Experimental Investigation of the Melting Process of Immiscible Binary Phase Change Materials *Heat Transfer Engineering* 44 2023: pp. 154–174. <https://doi.org/10.1080/01457632.2022.2034085>
14. **Sharma, M., Atheaya, D., Kumar, A.** Performance Evaluation of Indirect Type Domestic Hybrid Solar Dryer for Tomato Drying: Thermal, Embodied, Economical and Quality Analysis *Thermal Science and Engineering Progress* 42 2023: pp. 101882. <https://doi.org/10.1016/j.tsep.2023.101882>
15. **Abushanab, W.S., Zayed, M.E., Sathyamurthy, R., Moustafa, E.B., Elshiekh, A.H.** Performance Evaluation of a Solar Air Heater with Staggered/Longitudinal Finned Absorber Plate Integrated with Aluminium Sponge Porous Medium *Journal of Building Engineering* 73 2023: pp. 106841. <https://doi.org/10.1016/j.job.2023.106841>
16. **Bouhal, T., El Rhafiki, T., Kousksou, T., Jamil, A., Zeraouli, Y.** PCM Addition Inside Solar Water Heaters: Numerical Comparative Approach *Journal of Energy Storage* 19 2018: pp. 232–346. <https://doi.org/10.1016/j.est.2018.08.005>
17. **Kumar, A., Agrawal, R.** An Experimental Investigation of Cylindrical Shaped Thermal Storage Unit Consisting of Phase Change Material Based Helical Coil Heat Exchanger *Journal of Energy Storage* 45 2022: pp. 103795. <https://doi.org/10.1016/j.est.2021.103795>
18. **Mehrjardi, S.A.A., Khademi, A., Said, Z., Ushak, S., Chamkha, A.J.** Effect of Elliptical Dimples on Heat Transfer Performance in a Shell and Tube Heat Exchanger *Heat and Mass Transfer/Waerme- Und Stoffuebertragung* 59 2023: pp. 1781–1791. <https://doi.org/10.1007/s00231-023-03367-7>
19. **Ismail, I., Syahbana, M.S.L., Rahman, R.A.** Thermal Performance Assessment for an Active Latent Heat Storage Tank by Using Various Finned-Coil Heat Exchangers *International Journal of Heat and Technology* 40 2022: pp. 1470–1477. <https://doi.org/10.18280/ijht.400615>
20. **Salih, S.M., Jalil, J.M., Najim, S.E.** Experimental and Numerical Analysis of Double-Pass Solar Air Heater Utilizing Multiple Capsules PCM *Renewable Energy* 143 2019: pp. 1053–1066. <https://doi.org/10.1016/j.renene.2019.05.050>
21. **Hosseininaveh, H., Abadi, I.R., Mohammadi, O., Khademi, A., Shafii, M.B.** The Impact of Employing Carbon Nanotube and Fe<sub>3</sub>O<sub>4</sub> Nanoparticles Along with Intermediate Boiling Fluid to Improve the Discharge Rate of Phase Change Material *Applied Thermal Engineering* 215 2022: pp. 119032. <https://doi.org/10.1016/j.applthermaleng.2022.119032>
22. **Suyitno, B.M., Ismail, I., Rahman, R.A.** Improving the Performance of a Small-Scale Cascade Latent Heat Storage System by Using Gradual Melting Temperature Storage Tank *Case Studies in Thermal Engineering* 45 2023: pp. 103034. <https://doi.org/10.1016/j.csite.2023.103034>
23. **Ali, S., Mehrjardi, A., Khademi, A., Fazli, M.** Optimization of a Thermal Energy Storage System Enhanced with Fins Using Generative Adversarial Networks Method *Thermal Science and Engineering Progress* 49 2024: pp. 102471. <https://doi.org/10.1016/j.tsep.2024.102471>
24. **Xu, C., Xu, S., Eticha, R.D.** Experimental Investigation of Thermal Performance for Pulsating Flow in a Microchannel Heat Sink Filled with PCM (Paraffin/CNT Composite) *Energy Conversion and Management* 236 2021: pp. 114071. <https://doi.org/10.1016/j.enconman.2021.114071>
25. **Veismoradi, A., Ghalambaz, M., Shirivand, H., Hajjar, A., Mohamad, A., Sheremet, M., Chamkha, A., Younis, O.** Study of Paraffin-Based Composite-Phase

- Change Materials for a Shell and Tube Energy Storage System: A Mesh Adaptation Approach *Applied Thermal Engineering* 190 2021: pp. 116793.  
<https://doi.org/10.1016/j.applthermaleng.2021.116793>
26. **He, M., Xie, D., Yin, L., Gong, K., Zhou, K.** Influences of Reduction Temperature on Energy Storage Performance of Paraffin Wax/Graphene Aerogel Composite Phase Change Materials *Materials Today Communications* 34 2023: pp. 105288.  
<https://doi.org/10.1016/j.mtcomm.2022.105288>
  27. **Sawadogo, M., Godin, A., Duquesne, M., Lacroix, E., Veillère, A., Hamami, A.E.A., Belarbi, R.** Investigation of Eco-Friendly and Economic Shape-Stabilized Composites for Building Walls and Thermal Comfort *Building and Environment* 231 2023: pp. 110026.  
<https://doi.org/10.1016/j.buildenv.2023.110026>
  28. **Suyitno, B.M., Pane, E.A., Rahmalina, D., Rahman, R.A.** Improving the Operation and Thermal Response of Multiphase Coexistence Latent Storage System Using Stabilized Organic Phase Change Material *Results in Engineering* 18 2023: pp. 101210.  
<https://doi.org/10.1016/j.rineng.2023.101210>
  29. **Qu, Y., Wang, S., Zhou, D., Tian, Y.** Experimental Study on Thermal Conductivity of Paraffin-Based Shape-Stabilized Phase Change Material with Hybrid Carbon Nano-Additives *Renewable Energy* 146 2020: pp. 2637–2645.  
<https://doi.org/10.1016/j.renene.2019.08.098>
  30. **Lv, Y., Yang, X., Li, X., Zhang, G., Wang, Z., Yang, C.** Experimental Study on a Novel Battery Thermal Management Technology Based on Low Density Polyethylene-Enhanced Composite Phase Change Materials Coupled with Low Fins *Applied Energy* 178 2016: pp. 376–382.  
<https://doi.org/10.1016/j.apenergy.2016.06.058>
  31. **Al-Gunaid, T., Sobolčiak, P., Chriaa, I., Karkri, M., Mrlik, M., Ilčíková, M., Sedláček, T., Popelka, A., Krupa, I.** Phase Change Materials Designed from Tetra Pak Waste and Paraffin Wax as Unique Thermal Energy Storage Systems *Journal of Energy Storage* 64 2023: pp. 107173.  
<https://doi.org/10.1016/j.est.2023.107173>
  32. **Patil, J.R., Mahanwar, P.A., Sundaramoorthy, E., Mundhe, G.S.** A Review of the Thermal Storage of Phase Change Material, Morphology, Synthesis Methods, Characterization, and Applications of Microencapsulated Phase Change Material *Journal of Polymer Engineering* 43 2023: pp. 354–375.  
<https://doi.org/10.1515/polyeng-2022-0254>
  33. **Liu, C., Xiao, T., Zhao, J., Liu, Q., Sun, W., Guo, C., Ali, H.M., Chen, X., Rao, Z., Gu, Y.** Polymer Engineering in Phase Change Thermal Storage Materials *Renewable and Sustainable Energy Reviews* 188 2023: pp. 113814.  
<https://doi.org/10.1016/j.rser.2023.113814>
  34. **Sciacovelli, A., Navarro, M.E., Jin, Y., Qiao, G., Zheng, L., Leng, G., Wang, L., Ding, Y.** High Density Polyethylene (HDPE)-Graphite Composite Manufactured by Extrusion: A Novel Way to Fabricate Phase Change Materials for Thermal Energy Storage *Particuology* 40 2018: pp. 131–140.  
<https://doi.org/10.1016/j.partic.2017.11.011>
  35. **Firman, L.O.M., Rahmalina, D., Ismail, I., Rahman, R.A.** Hybrid Energy-Temperature Method (HETM): A Low-Cost Apparatus and Reliable Method for Estimating the Thermal Capacity of Solid–Liquid Phase Change Material for Heat Storage System *HardwareX* 16 2023: pp. e00496.  
<https://doi.org/10.1016/j.ohx.2023.e00496>
  36. **Shamseddine, I., Pennec, F., Biwole, P., Fardoun, F.** Supercooling of Phase Change Materials: A Review *Renewable and Sustainable Energy Reviews* 158 2022: pp. 112172.  
<https://doi.org/10.1016/j.rser.2022.112172>



© Rahman et al. 2024 Open Access This article is distributed under the terms of the Creative Commons Attribution 4.0 International License (<http://creativecommons.org/licenses/by/4.0/>), which permits unrestricted use, distribution, and reproduction in any medium, provided you give appropriate credit to the original author(s) and the source, provide a link to the Creative Commons license, and indicate if changes were made.